PHYSICAL REVIEW E **83**, 031909 (2011)

Oscillation propagation in neural networks with different topologies

Yang Gao[*] and Jianjun Wang

College of Nuclear Science and Technology, Harbin Engineering University, Harbin 150001, China

(Received 3 October 2010; published 17 March 2011)

In light of the issue of oscillation propagation in neural networks, various topologies of FitzHugh-Nagumo neuron populations are investigated. External Gaussian white noise is injected into the first neuron only. Before the oscillation spreads to the other neurons in the network, some of the inherent stochasticity within the noise-induced oscillation of the first neuron is filtered out due to the neuron's nonlinear dynamics. Both the temporal and the spatial coherence of the evoked activity's propagation are analyzed in conjunction with the network topology randomness p, the coupling strength between neurons g, and the noise amplitude D. The temporal periodicity of the global neural network presents a typical coherence biresonance (CBR) characteristic with regard to the noise intensity. The network topology randomness exerts different influences on the resonance effects for different coupling strength regimes. At an intermediate coupling strength, the random shortcuts reinforce the interactions between the neurons, and then more stochasticity in the firings of the first neuron spreads within the network. Consequently, CBR is decreased with the increase of the network topology randomness. At a large coupling strength, the random shortcuts assist the nonlinearity in impairing the stochastic components, and consequently help to enhance the resonance effects, which differed significantly from previous related work. However, the degree of the spatial synchronization of the systems increases monotonically as the network topology randomness increases at any coupling strength.

DOI: 10.1103/PhysRevE.83.031909 PACS number(s): 87.18.Sn, 87.10.−e

I. INTRODUCTION

Excitability is a common property of many systems in nature, such as the retina [1], heart tissues [2], aggregating amoebae [3], and the Belousov-Zhabotinsky (BZ) reaction [4,5]. Excitable systems have only one stable steady state but are highly sensitive to perturbations. Perturbations above a small threshold can make an excitable system undergo large excursions in phase space before eventually returning to the original rest state. Neurons, an important class of excitable systems, are constitutive elements of the biological brain [6]. In a neural system, when perturbation is imposed on one neuron, spikes are accordingly generated in the neuron and transmitted to other neurons by means of synaptic coupling. Most neurons communicate with each other by the means of spike trains, which is believed to support information processing in the brain. In recent years, many investigations have been devoted to the propagation of excitation between neurons. For instance, the mean and standard deviation, as well as the coefficient of variation, of the interspike intervals in the second element have been studied when three kinds of noise are added to the first element in a coupled excitable system through both a computer simulation and a circuit experiment [7]; Rosa *et al.* [8] have observed the arising of a new slow regular rhythm along a chain of Hindmarsh-Rose neurons which are coupled by inhibitory connections; Li *et al.* [9] have reported the spatiotemporal dynamics of coupled FitzHugh-Nagumo neurons and found that noise-induced oscillation of the first neuron is propagated along the chain with noise suppression. However, in these studies, the connections between the neurons are one-way or unidirectional. It is known that a real neural system, as well as many other systems, exhibits much more complex connectivity.

Many systems composed of dynamical units can be described by networks with nodes representing units and edges representing interactions among units [10]. The neural network of the worm *Caenorhabditis elegans*, the power grid of the western United States, and the collaboration graph of film actors have all been shown to share some common "small-world" network characteristics [11]. The small-world network, proposed by Watts and Strogatz in 1998, stands for a network interpolating between a regular network and a completely random network and was developed in an effort to understand the high degree of coordination in cricket chirps. The two main properties of such a small-world network are that it has a large clustering coefficient like a regular network, while at the same time having a short characteristic path length similar to a completely random network. The clustering coefficient is defined as the extent to which nodes connected to any node in a network are connected to each other. The characteristic path length represents the number of edges in the shortest path between two nodes of a network, averaged over all node pairs. The topological properties of small-world networks and the effects of small-world topology on dynamical behavior in nonlinear networks have been studied intensively [12–17]. For example, it has been reported that a localized transient stimulus results either in self-sustained persistent activity or in a brief transient followed by failure at low densities of directed random connections in a small-world integrate-and-fire neuron network [14]. It has been shown that a small-world network is efficient for information exchange [15] and can enhance the efficiency of associated memory [16]; the storage capacity and the retrieval time of Hopfield-type neural networks for four network structures, including small-world network structure, have also been studied in detail [17].

It is a fact that real neurons are usually exposed to external or inherent noise and work in noisy conditions. Noise plays an important role in the dynamical behavior of neurons. At an optimal noise intensity the regularization of noise-induced

---

[*] Corresponding author. FAX: +86-451-8256-9655; gaoyang@hrbeu.edu.cn

response in the form of spike trains is maximized in a neural system without an external drive, which is known as coherence resonance (CR) [18]. Experimental evidence of CR has been reported in the coherence between spinal and cortical neurons in the somanosensory system of an anesthetized cat [19]. In this study, the constructive role of noise is discussed concerning networks composed of FitzHugh-Nagumo (FHN) excitable cells with varying topological structures, where only the first neuron is subject to the external noise. The results show that noise-induced oscillation of the first neuron can be transmitted to the others with noise suppression. The specific propagation case in each neuron depends strongly on the coupling between neurons and the network topology. The temporal coherence of the network presents a typical coherence biresonance characteristic. Increasing randomness of the network structure decreases the temporal coherence at not large coupling strength, while it promotes the spatial synchronization of the networks at any coupling.

II. MODEL DESCRIPTION

The model used here consists of FHN neurons in which a small-world network topology is constructed as follows. First, a regular ring of N neurons is considered, and each neuron connects to its nearest k neighbors by undirected edges; thus, there are $\frac{1}{2}Nk$ edges in the entire graph. A neuron is selected at random as the first neuron and the other neurons are marked clockwise by their numbers. Next, each edge is visited once and, with the rewiring probability p, removed and reconnected to a randomly chosen neuron. It should be noted that many network realizations exist for a given p. Herein, that $N = 100$ and $k = 4$ is set, and p takes different values between 0 and 1. For clarity, taking $N = 40$ and $k = 4$ as an example, three realizations of this process for different values of p are shown in Fig. 1. For $p = 0$, only local connections are present; the graph becomes more random with the increase of p until $p = 1$; any two neurons in the network are connected with the same probability (global connectivity). The FHN model investigated in this work is simplified from the Hodgkin-Huxley (HH) model and is amenable to analysis, although it does not have as firm an experimental basis as the HH model. The FHN model has been widely used in neuroscience to study various neural activities, such as spiral waves [20], synchronization [21], stochastic resonance [22,23], and CR [24,25]. The dynamics of the FHN neuron are described by the following equations:

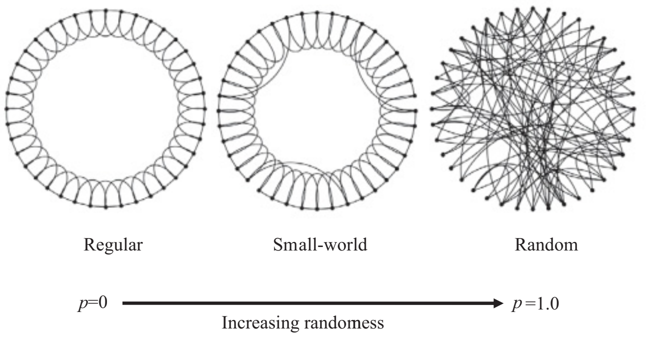

FIG. 1. The illustration of network topology transformation, starting from a regular network via a small-network network to a completely random network.

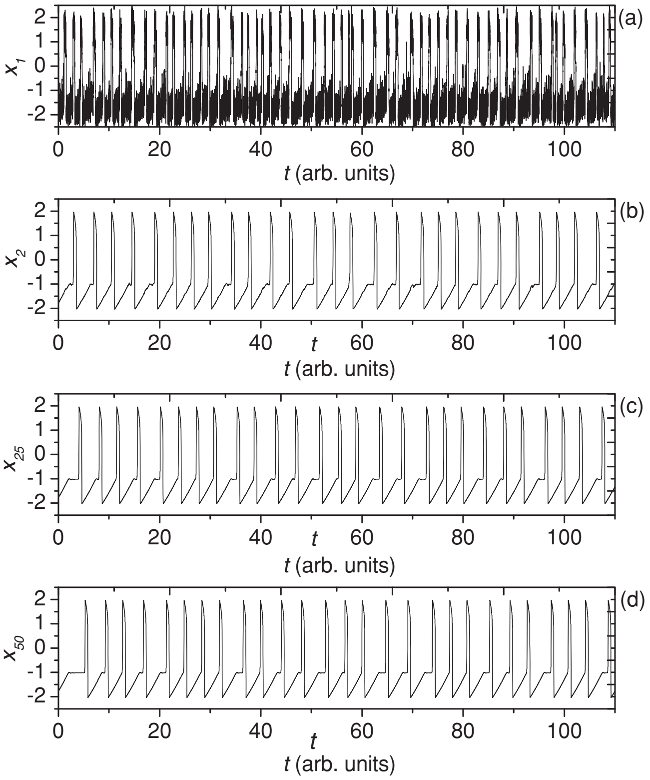

FIG. 2. The time series of x_1,x_2,x_{25}, and x_{50} at $\varepsilon = 0.01$, $a = 1.02$, $p = 0$, $g = 0.01$, and $D = 0.05$.

$$\varepsilon\frac{dx_i}{dt} = x_i - \frac{x_i^3}{3} - y_i + g_{ij}(x_j - x_i), \tag{1}$$

$$\frac{dy_i}{dt} = x_i + a_i. \tag{2}$$

Here i and j running from 1 to N are the numbers of the neurons. $x_i(t)$ is a fast voltage variable representing the membrane voltage of the ith neuron, and $y_i(t)$ is a slow

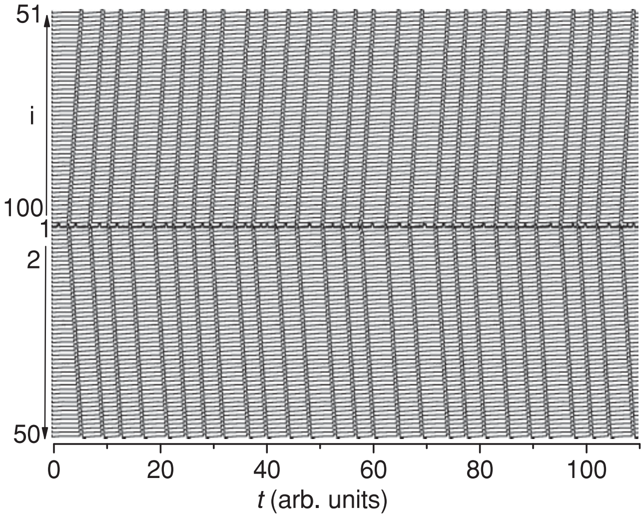

FIG. 3. The spatiotemporal evolution of all 100 neurons at $\varepsilon = 0.01$, $a = 1.02$, $p = 0$, $g = 0.01$, and $D = 0.05$.

recovery variable. The time constant $\varepsilon = 0.01$ determines the speed of the firing process. The parameter a_i is a control parameter of the ith neuron. For a single FHN model, if $|a_i| > 1$, the system only has a stable fixed point, whereas if $|a_i| < 1$ then a limit cycle appears. The system with fixed-point dynamics ($|a_i|$ slightly larger than unity) is excitable because it will return to the fixed point only after a large excursion when perturbed away from the fixed point. Herein, a_i, the control parameter, is set to 1.02 and is supposed to be the same for each neuron. g_{ij} is the coupling parameter between the two neurons i and j, and its value is determined by the coupling pattern of the system. If these two neurons are coupled to each other, g_{ij} is a determinate value g; otherwise, $g_{ij} = 0$. When a noise source term is inserted into Eq. (1) of the first neuron, the dynamical equations of the first neuron are as follows:

$$\varepsilon \frac{dx_1}{dt} = x_1 - \frac{x_1^3}{3} - y_1 + g_{1j}(x_j - x_1) + \xi(t), \tag{3}$$

$$\frac{dy_1}{dt} = x_1 + a_1, \tag{4}$$

where $\xi(t)$ is Gaussian white noise with $\langle \xi(t) \rangle = 0$, and $\langle \xi(t)\xi(t') \rangle = 2D\delta(t - t')$. D is the strength of $\xi(t)$.

III. RESULTS AND DISCUSSION

The differential equations (1)–(4) are numerically integrated using the Euler scheme with a fixed time step of 0.002. Figures 2(a)–2(d) show the time series of x_1,x_2,x_{25}, and x_{50}, respectively. Spikes are generated in these four neurons. The dispersion of the interspike intervals of x_1 is less regular than for the others and the oscillation amplitude of x_1 is slightly larger compared with the other neurons. It is indicated that noise-induced oscillation of the first neuron transmits to the others by coupling with noise suppression. The spatiotemporal evolution of the membrane voltage of all 100 neurons in the network is shown in Fig. 3.

To quantitatively characterize the temporal coherence of the firings in a neuron, the coherence factor R_i of the oscillation of the variable x_i is obtained by the following formula:

$$R_i = \frac{\sqrt{\mathrm{var}\,(T_k)}}{\langle T_k \rangle}. \tag{5}$$

Here $T_k = t_{k+1} - t_k$, and t_k is the time of the kth pulse in the time series of x_i. A smaller R_i corresponds to a better spiking regularity. This quantity is of biological importance because it is related to the timing precision of the information processing in neural systems [26]. Note that a pulse occurs

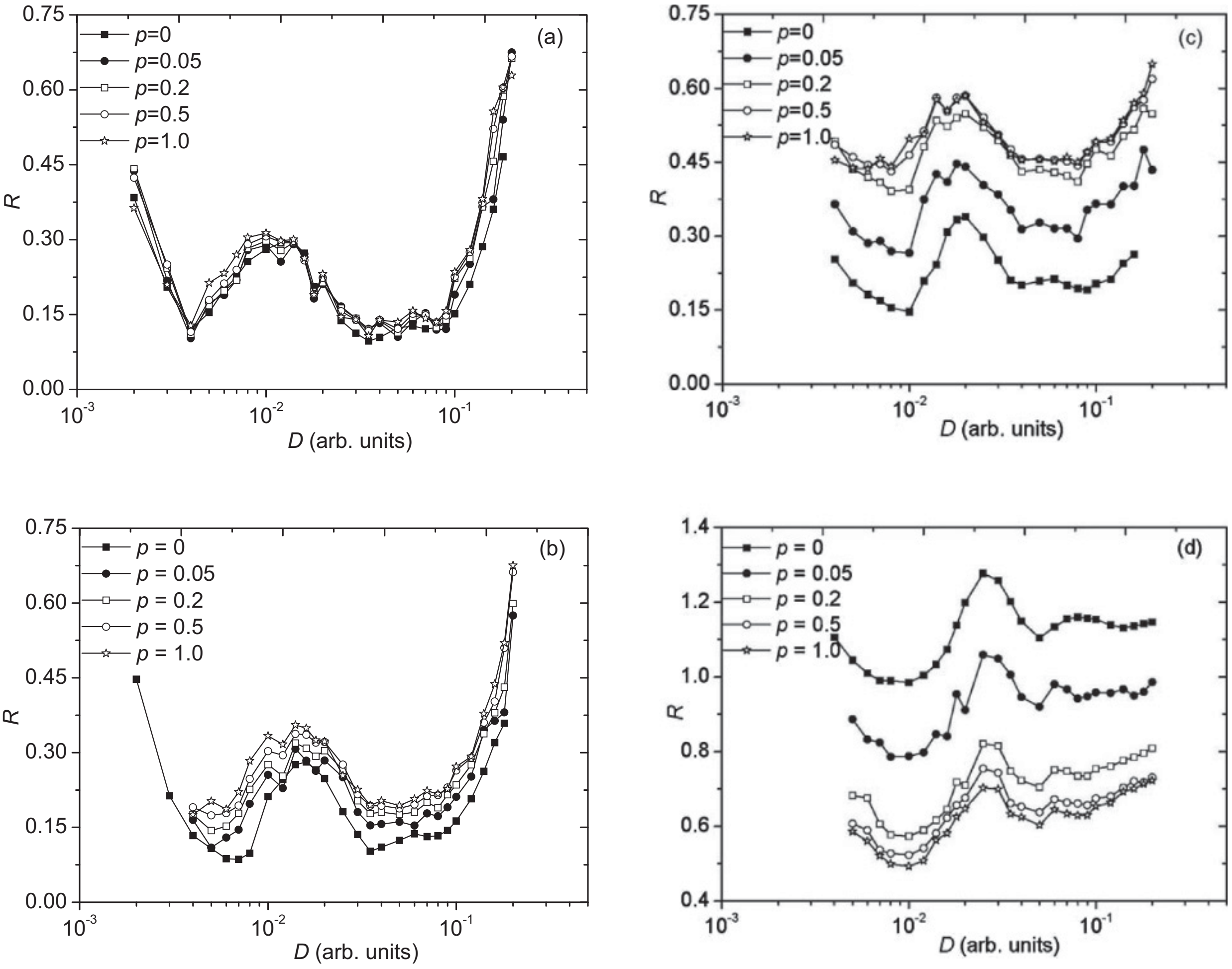

FIG. 4. The coherence factor R versus the noise intensity D at different rewiring probabilities p with (a) $g = 0.0075$; (b) $g = 0.01$; (c) $g = 0.015$; (d) $g = 0.03$. $\varepsilon = 0.01$, $a = 1.02$.

when the state variable x exceeds a certain threshold value x_0 (here taken arbitrarily as $x_0 = 1.0$) and it turns out that the threshold value can vary in a wide range without altering the results. The temporal coherence of the whole network is measured by the average factor R,

$$R = [\langle R_i \rangle], \tag{6}$$

where $\langle\cdot\rangle$stands for the average of all the neurons except for the first one and $[\cdot]$ denotes averaging over 30 different network realizations for each p.

To measure the spatial synchronization of the system quantitatively, the standard deviation σ is defined as in Eq. (7):

$$\sigma = [\langle \sigma(t) \rangle], \quad \sigma(t) = \sqrt{\frac{\left[\frac{1}{N}\sum_{i=1}^{N} x_i(t)^2 - \left\{\frac{1}{N}\sum_{i=1}^{N} x_i(t)\right\}^2\right]}{(N-1)}}, \tag{7}$$

where $\langle\cdot\rangle$ stands for the average over time and $[\cdot]$ has the same meaning as in Eq. (6). Larger $\sigma(t)$ corresponds to larger deviation between the neurons, and smaller $\sigma(t)$ represents better synchronization.

Figures 4(a)–4(d) plot the coherence factor R against the input noise intensity D achieved at different rewiring probabilities p and coupling strengths g. Each curve in Figs. 4(a)–4(d) presents a typical coherence biresonance (CBR) characteristic; that is, two optimal coherence factors, R_{opt1} and R_{opt2}, exist which correspond to two optimal noise intensities, D_{opt1} and D_{opt2}, respectively. When $g = 0.0075$, the curves trend to overlap, indicating that the effect of the topological structure on the system's dynamical behavior is feeble at a weak coupling strength. When g increases to 0.010, one can see that the two minima of R rise as the rewiring probability p increases, which suggests that the increase of the disorder of the network plays a negative role in enhancing CBR under these circumstances. When the coupling strength increases further to $g = 0.015$ [see Fig. 4(c)], the damaging effect of the randomness of the network on the spiking regularity of the neurons becomes more obvious compared to Fig. 4(b). It is shown that CBR is greatly suppressed in the case of $p = 0.05$. With the increase of the network topology randomness (see the curves for $p = 0.20$ and $p = 0.50$), CBR is decreased even more. However, when the network becomes completely random ($p = 1.0$), CBR is not decreased any further and the corresponding curve almost overlaps with the one representing $p = 0.50$. The dynamical behavior of the neurons at $g = 0.030$ clearly differs from those at the other three coupling intensities. As shown in Fig. 4(d), increasing the disorder of the network enhances CBR instead of suppressing it. However, when comparing the values of R_{opt1} and R_{opt2} at the same rewiring probability but different coupling strengths, it is obvious that R_{opt1} and R_{opt2} are the largest at $g = 0.030$, as shown in Fig. 5.

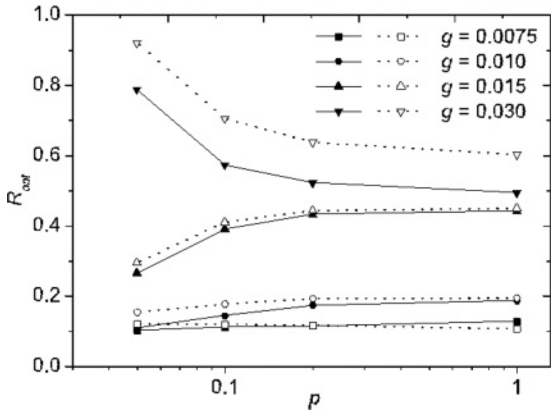

FIG. 5. The optimal coherence factors R_{opt1} (solid lines) and R_{opt2} (dotted lines) versus the rewiring probability p at different coupling strengths at $\varepsilon = 0.01$, $a = 1.02$.

Combining the viewpoints of Li and Lang [9] and Miyakawa *et al.* [27], the oscillation propagation phenomenon above might be understood in this way: The original firings transmitted from the first neuron to the others are more or less irregular; however, the nonlinearity of the neurons can act as a "filter" and eliminate partly stochastic components in the firings. Therefore, the coherence of the firings in other neurons increases as a result of the cooperation of the coupling and nonlinearity. Of course, the transmission instances differ when considering various network topologies and coupling strength regimes. When the coupling strengths are intermediate such as $g = 0.01$, in a regular network, except that the coherence of the firings in the neuron closest to the first one is excessively poor at strong noise intensities, the firings exhibit relatively periodic activity, as shown in the solid lines in Fig. 6(a). Figure 6(b) denotes a case with small-world topology ($p = 0.2$); it can be seen that the whole CBR effect decreases compared with that of when $p = 0$, which is reflected more clearly in completely random networks [see the solid lines in Fig. 6(c)]. This behavior can be explained by the $L(p)$-p plot in Fig. 7. The characteristic path length $L(p)$ decreases rapidly as p increases; thus, the first neuron could potentially have a higher number of "close neighbors" and then take this opportunity to spread more stochastic components to the neural network. Consequently, with the increase of the network topology randomness, the overall CBR of the system is reduced at the intermediate coupling strengths.

In the case of strong coupling, that is, $g = 0.03$, the neurons' interaction is enhanced and the other neurons tend to show the dynamical behavior more similar to the first neuron. In a regular neural network, it can be observed from the dotted lines in Fig. 6(a) that, except for the neuron farthest from the first one, the coherence factors of most neurons at any noise intensity are large; even the curve of R_2 versus D simply presents CR instead of CBR characteristics. In networks with small-world topology, improved CBR or CR is demonstrated in most neurons, and CBR of the neuron farthest apart from the first one decreases inversely. In the case of $p = 1$, the integrated resonance effects are optimal in the three sets of dotted lines in Figs. 6(a) to 6(c), which is consistent with the fact that the temporal coherence of the collective firings is enhanced with the increase of the disorder of the network topological structure in Fig. 4(d).

From the plots in Fig. 6 it can be found that long-range connection in the systems has the opposite impact on the resonance effects in different coupling strength regimes. When the coupling strength is not large, the random shortcuts reinforce the interactions between neurons. As a result, more stochasticity in the firings is transmitted from the first neuron

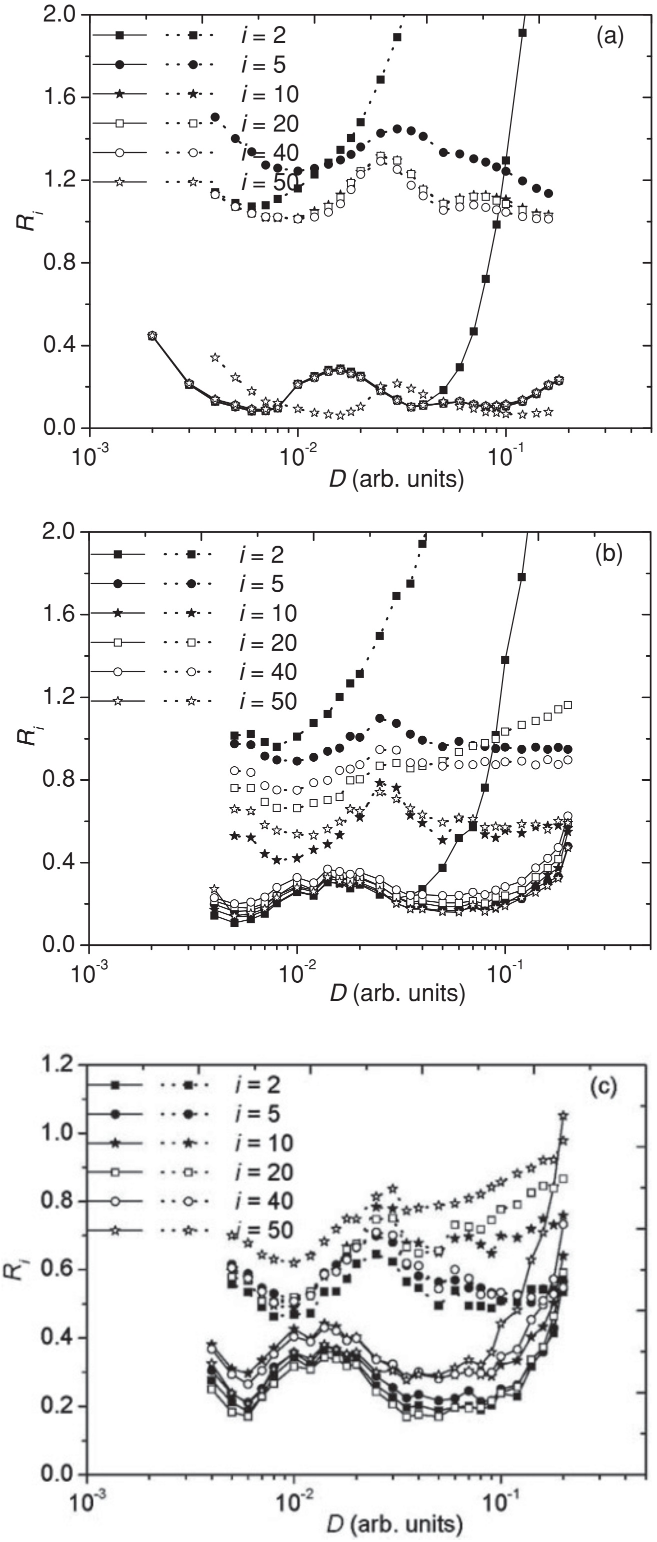

FIG. 6. The coherence factor R_i versus the noise intensity D at two different coupling strengths (solid line $g = 0.01$, and dotted line $g = 0.03$) with (a) $p = 0$; (b) $p = 0.2$; (c) $p = 1.0$. $\varepsilon = 0.01$, $a = 1.02$.

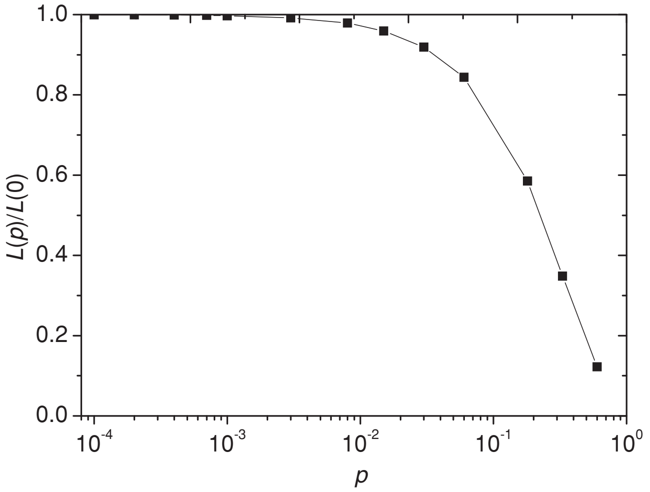

FIG. 7. Characteristic path length L as a function of the rewiring probability p for WS small-world networks with $N = 100$ and $K = 4$. It is normalized by each value at $p = 0$.

to the others, and the collective coherence motion is suppressed with the increase of the rewiring probability p. In the case of strong coupling, all the neurons tend to behave as a single one, and the random shortcuts, in turn, assist the nonlinearity in filtering out some stochastic components in the firings of the first neuron. Therefore, randomness of the network topology plays a positive role in enhancing the resonance effects of the neurons at $g = 0.030$.

In order to better understand the global dynamical behavior of the neural networks with different topological structures, while still considering cases of $g = 0.010$ and $g = 0.030$ as examples, the dependence of R_i on i for various noise intensities in regular, small-world, and completely random networks is portrayed in Figs. 8 and Figs. 9, respectively. In Fig. 8(a), at low levels of noise ($D = 0.004$ and $D = 0.006$), the further the ith neuron is away from the first one, the worse the coherence of the firings. At moderate noise intensities ($D = 0.020$ and $D = 0.035$), noise-induced oscillation of the first neuron propagates along both sides with slightly improved coherence. At a high noise level ($D = 0.100$), unless the coherence of the firings in the neurons closest to the first one is seriously damaged, the law of oscillation transmission to other neurons functions similarly to situations involving the weak noise intensities. In a neural network with small-world topological structure, it can be seen from Fig. 8(b) that R_i as a function of i is disordered and fluctuating regardless of the noise strength. In a completely random network, the value of the coherence factor R_i demonstrates larger ups and downs, as shown in Fig. 8(c). In addition, most of R_i in the plots of Figs. 8(b) and 8(c) is larger than shown in Fig. 8(a) at a fixed noise intensity. The cases for $g = 0.0075$ and $g = 0.015$ (not shown) are similar to that for $g = 0.010$, whereas the difference between the values of R_i at the same noise strength is smaller for the former, and is larger for the latter compared to that when $g = 0.010$.

In the case of $g = 0.030$, the curves of R_i versus i are very different from those for when $g = 0.010$. In a regular neural network, unless the coherence of the firings in the neurons in the vicinity of the first one is destroyed significantly, R_i first decreases very slowly and then suddenly declines rapidly with an increase of the distance from the ith neuron to the first one, as depicted in Fig. 9(a). Moreover, most of the values of R_i are very high, and only the regularity of the firings in the neurons farthest from the first one is preferable. In the plots of

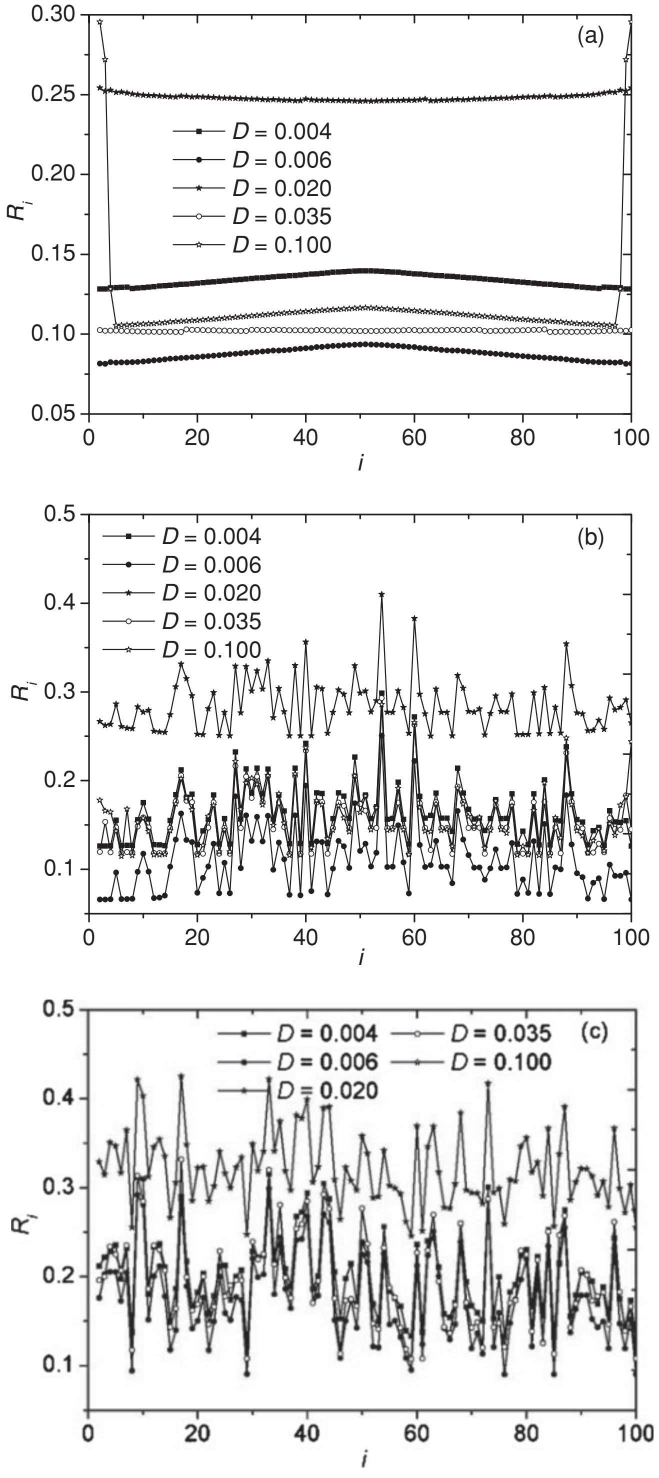

FIG. 8. The coherence factor R_i versus the neuron number i at different noise intensities D with (a) $p = 0$; (b) $p = 0.05$; (c) $p = 1.0$. $\varepsilon = 0.01$, $a = 1.02$, $g = 0.01$.

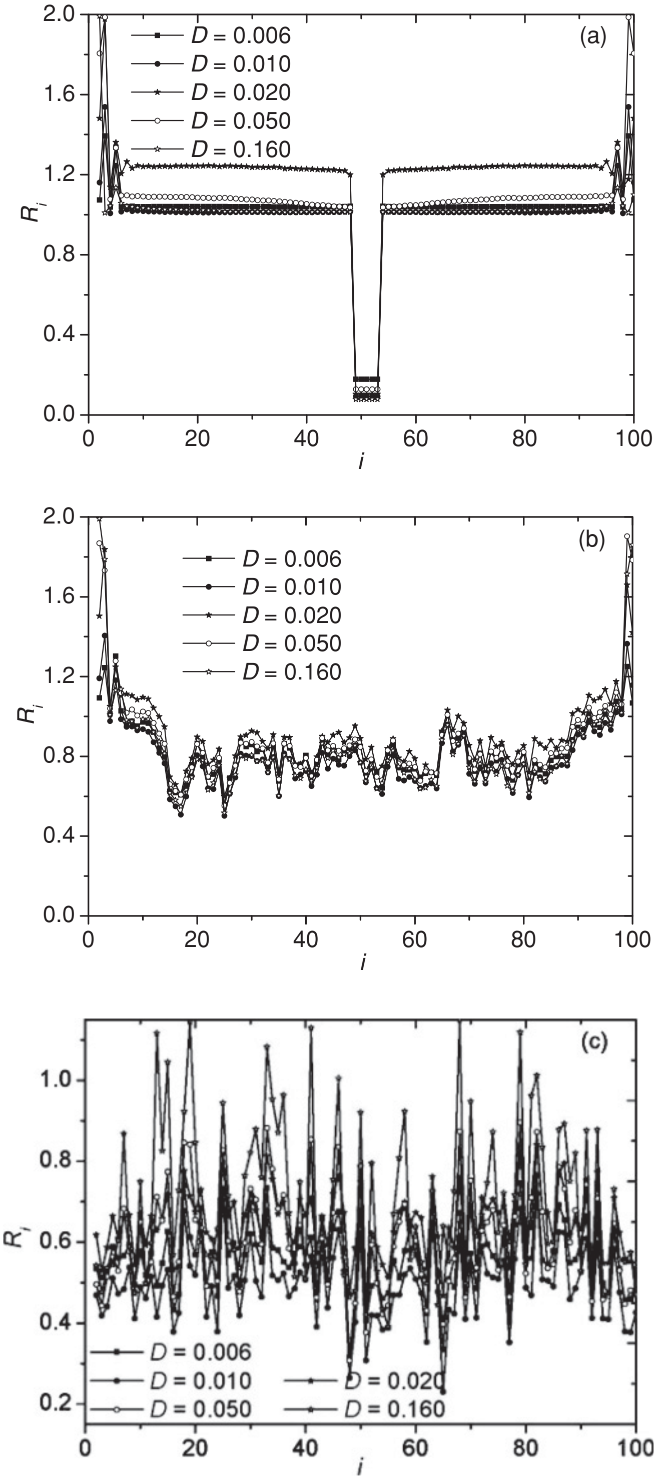

FIG. 9. The coherence factor R_i versus the neuron number i at different noise intensities D with (a) $p = 0$; (b) $p = 0.05$; (c) $p = 1.0$. $\varepsilon = 0.01$, $a = 1.02$, $g = 0.03$.

Figs. 9(b) and 9(c), R_i begins to fluctuate, and the fluctuation range increases with the network topology, changing from small-world to completely random. Furthermore, the symbols representing R_i at different noise intensities in the two plots mingle together, implying that the effects of the external noise is weakened. At this moment the main role of the external noise is as an "igniter" and the characterizations of the firings in each neuron are less influenced by the noise intensity.

Figures 10(a) to 10(d) depict how the spatial coherence between neurons changes with the noise intensity at various rewiring probabilities p and coupling strengths g. It is interesting to note that similar to the curve of R versus D,

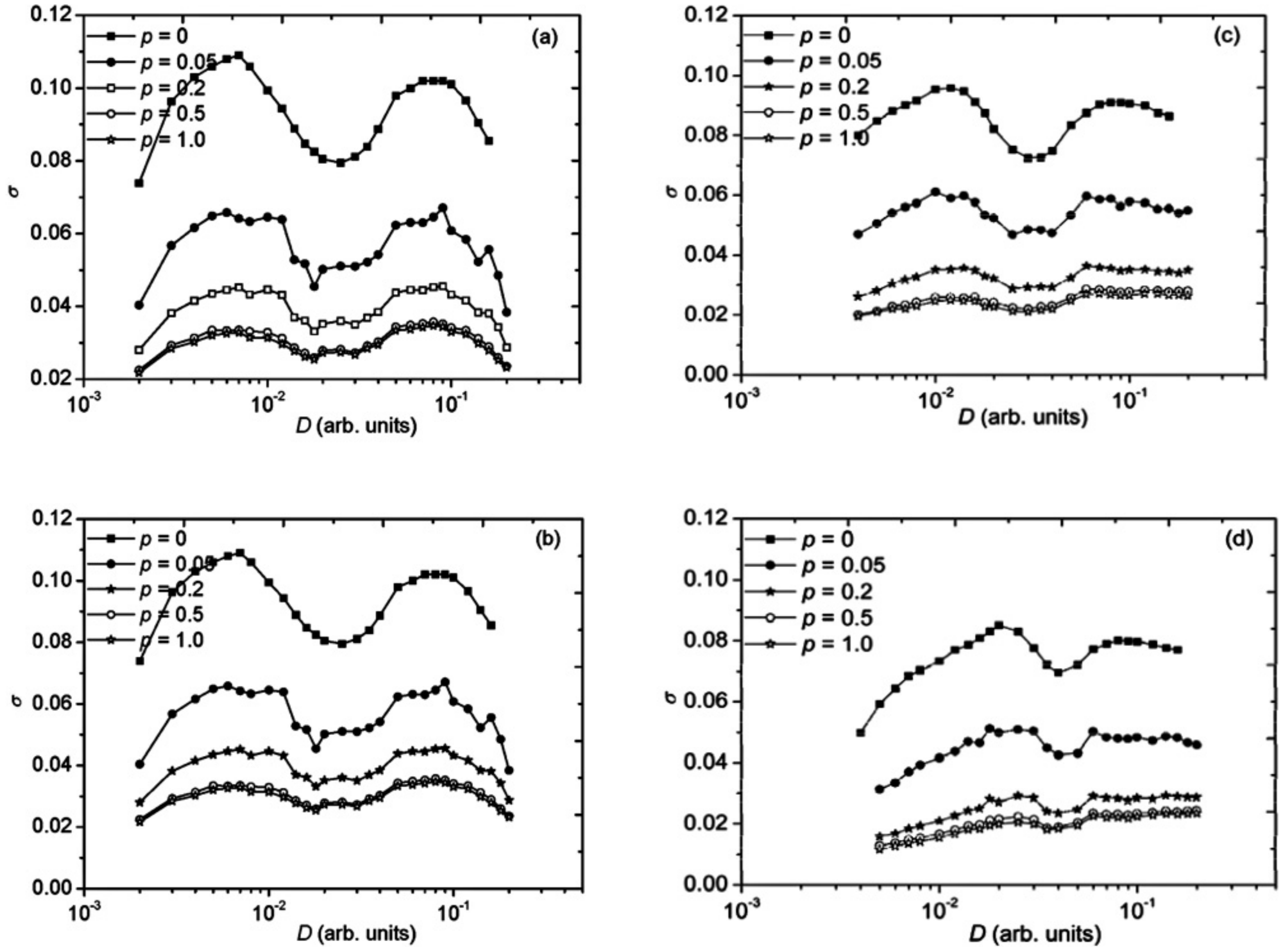

FIG. 10. The standard deviation σ versus the noise intensity D at different rewiring probabilities p with (a) $g = 0.0075$; (b) $g = 0.01$; (c) $g = 0.015$; (d) $g = 0.03$. $\varepsilon = 0.01$, $a = 1.02$.

each curve of σ against D has two extrema. The difference lies in the fact that the two minimums of R represent the optimal temporal coherence, while the two maximums of σ stand for the worst spatial synchronization. Moreover, it can be observed that at a fixed noise intensity, σ decreases monotonically as p increases regardless of the coupling strength, which is similar to the findings of several previous studies [28,29]. Comparing the four plots in Fig. 10, it can be found that the system becomes more synchronized as the coupling strength g becomes larger. Therefore, strengthening the coupling between neurons or adding random shortcuts in the system is an effective way for the system to achieve a periodic spatial state.

IV. SUMMARY

In this paper, numerical simulations are presented for both population and individual dynamical behavior of an array of coupled FitzHugh-Nagumo neurons with various topological networks. It is demonstrated that noise-induced oscillation of the first neuron can be transmitted to the others with noise suppression. The transmission instances are strongly dependent on the network topology and the coupling strength. At not very high levels of coupling, in a regular network the coherence of the firings in a neuron is gradually improved as the distance from this neuron to the first one increases, and the coherence factor R_i as a function of the number of the neuron i demonstrates highs and lows in small-world and completely random networks. In the case of strong coupling, the regularity of the firing in the neurons is mostly destroyed as a whole. The temporal coherence of the systems presents a typical coherence biresonance characteristic. Increasing the randomness of the network topology plays a negative role in enhancing coherence biresonance at an intermediate coupling strength, which is opposite to the situation at a strong coupling strength. The worst spatial synchronization of the neurons appears twice in the selected range of the noise intensity, and the spatial coherence improves with the increase of the disorder of the network topology and the coupling strength.

Unlike some previous results [30,31], the phenomenon of CBR instead of CR occurs in the neural networks. Moreover, the temporal coherence of the networks does not show any superiority but instead some disadvantages as a whole when introducing long-range connection into the original regular networks. The basic reason for this situation is that each neuron is subject to an independent source of noise in those cases, while the external noise is only injected to the first neuron here. The study reconfirms that the brain is a complex and fascinating processor and that the neuron activity in the brain is controlled by many factors such as the noise intensity, the procedure of introducing a noise, the coupling between neurons, and the network topology. The influence of each control factor on the dynamical behavior of the neural networks is unique on the one hand and modulated by the other factors on the other hand. These individual factors constitute an integrated system, and the neural networks show different dynamical characteristics under the interplay of these factors. It is anticipated that these results will provide further insight into information transmission and processing taking place in real neural systems.

ACKNOWLEDGMENTS

The work was supported by School Fund of Harbin Engineering University (002150260705).

[1] Markus A. Dahlem and S. C. Müller, Exp. Brain Res. **115**, 319 (1997).
[2] G. Bub, A. Shrier, and L. Glass, Phys. Rev. Lett. **88**, 058101 (2002).
[3] E. Pálsson and E. C. Cox, Proc. Natl. Acad. Sci. USA **93**, 1151 (1996).
[4] A. N. Zaikin and A. M. Zhabotinsky, Nature **225**, 535 (1970).
[5] A. T. Winfree, Science **175**, 634 (1972).
[6] R. Guantes and Gonzalo G. de Polavieja, Phys. Rev. E **71**, 011911 (2005).
[7] Yo Horikawa, Phys. Rev. E **64**, 031905 (2001).
[8] M. La Rosa, M. I. Rabinovich, R. Huerta, H. D. I. Abarbanel, and L. Fortuna, Phys. Lett. A **266**, 88 (2000).
[9] Q. Li and X. Lang, Phys. Rev. E **74**, 031905 (2006).
[10] R. Albert and A.-L. Barabási, Rev. Mod. Phys. **74**, 47 (2002).
[11] D. J. Watts and S.H. Strogatz, Nature (London) **393**, 440 (1998).
[12] A. R. Atilgan, P. Akan, and C. Baysal, Biophys. J. **86**, 85 (2004).
[13] F. Jasch and A. Blumen, J. Chem. Phys. **117**, 2474 (2002).
[14] A. Roxin, H. Riecke, and S. A. Solla, Phys. Rev. Lett. **92**, 198101 (2004).
[15] D. H. Zanette and M. Kuperman, Physica A **309**, 445 (2002).
[16] L. G. Morelli, G. Abramson, and M. Kuperman, Eur. Phys. J. B **38**, 495 (2004).
[17] H. Oshima and T. Odagaki, Phys. Rev. E **76**, 036114 (2007).
[18] A. S. Pikovsky and J. Kurths, Phys. Rev. Lett. **78**, 775 (1997).
[19] E. Manjarrez, J. G. Rojas-Piloni, I. Méndez, L. Martínez, D. Vélez, D. Vázquez, and A. Flores, Neurosci. Lett. **326**, 93 (2002).
[20] X. Wang, Y. Lu, M. Jiang, and Q. Ouyang, Phys. Rev. E **69**, 056223 (2004).
[21] H. Hasegawa, Phys. Rev. E **70**, 066107 (2004).
[22] D. Nozaki, J. J. Collins, and Y. Yamamoto, Phys. Rev. E **60**, 4637 (1999).
[23] D. Nozaki and Y. Yamamoto, Phys. Lett. A **243**, 281 (1998).
[24] O. Kwon, H. H. Jo, and H. T. Moon, Phys. Rev. E **72**, 066121 (2005).
[25] P. Gong, J. Xu, and S. Hu, Chaos, Solitons Fractals **13**, 885 (2002).
[26] X. Pei, L. Wilkens, and F. Moss, Phys. Rev. Lett. **77**, 4679 (1996).
[27] K. Miyakawa, T. Okano, and T. Tanaka, Phys. Rev. E **71**, 066202 (2005).
[28] Z.Gao, B. Hu, and G. Hu, Phys. Rev. E **65**, 016209 (2001).
[29] Y. Gong, B. Xu, Q. Xu, C. Yang, T. Ren, Z. Hou, and H. Xin, Phys. Rev. E **73**, 046137 (2006).
[30] Q. Li and Y. Gao, Biophys. Chem. **130**, 41 (2007).
[31] Q. Li and Y. Gao, Phys. Rev. E **77**, 036117 (2008).